Article

Self-Immobilized Putrescine Oxidase Biocatalyst System Engineered with a Metal Binding Peptide

Nilan J. B. Kamathewatta, Dwight O'Dell Deay, Banu Taktak Karaca, Steve A. Seibold, Tyler M. Nguyen, Brandon Tomas, Mark L Richter, Cindy L Berrie, and Candan Tamerler

Langmuir, **Just Accepted Manuscript** • DOI: 10.1021/acs.langmuir.0c01986 • Publication Date (Web): 12 Sep 2020

Self-Immobilized Putrescine Oxidase Biocatalyst System Engineered with a Metal Binding Peptide

Nilan J. B. Kamathewatta‡[a], Dwight O. Deay III‡[b], Banu Taktak Karaca[c,d], Steve Seibold[b], Tyler M. Nguyen[a], Brandon Tomás[c,f], Mark L. Richter[b], Cindy L. Berrie[a,c], Candan Tamerler*[c,e,f]*

[a]Department of Chemistry; University of Kansas, Lawrence, KS 66045, USA

[b]Department of Molecular Biosciences; University of Kansas, Lawrence, KS 66045, USA

[c]Institute for Bioengineering Research, University of Kansas, Lawrence, KS 66045, USA

[d]Department of Molecular Biology and Genetics, Biruni University, İstanbul, Turkey, 34010

[e]Bioengineering Program, University of Kansas, Lawrence, KS 66045, USA

[f]Department of Mechanical Engineering, University of Kansas, Lawrence, KS 66045, USA

*Corresponding authors: Cindy L. Berrie (cberrie@ku.edu), Candan Tamerler (ctamerler@ku.edu)

‡ equally contributed, co-first authors

Key Words: putrescine oxidase, enzyme immobilization, flavin oxidases, gold binding peptide; biocatalysts; self-assembly

Running Title: Engineered putrescine oxidase enzyme self-immobilizes on gold surfaces

Abstract

Flavin oxidases are valuable biocatalysts for the oxidative synthesis of a wide range of compounds, while at the same time reducing oxygen to hydrogen peroxide. Compared to other redox enzymes, their ability to use molecular oxygen as an electron acceptor offers a relatively simple system which does not require a dissociable coenzyme. As such, they are attractive targets for adaptation as cost effective biosensor elements. Their functional immobilization on surfaces offers unique opportunities to expand their utilization for a wide range of applications. Genetically engineered peptides have been demonstrated as enablers of the functional assembly of biomolecules at solid materials interfaces. Once identified as having a high affinity for the material of interest, these peptides can provide a single step bio-assembly process with orientation control, a critical parameter for functional immobilization of the enzymes. In this study, for the first time, we explored bio-assembly of a putrescine oxidase enzyme using a gold binding peptide tag. The enzyme was genetically engineered to incorporate a gold binding peptide with an expectation of effective display of the peptide tag to interact with the gold surface. In this work, the functional activity and expression were investigated, along with the selectivity of the binding of the peptide tagged enzyme. The fusion enzyme was characterized using multiple techniques including protein electrophoresis, enzyme activity, microscopic and spectroscopic methods to verify functional expression of the tagged protein with near native activity. Binding studies using quartz crystal microbalance (QCM), nanoparticle binding studies, and atomic force microscopy studies were used to address the selectivity of the binding through the peptide tag. Surface binding AFM studies show that the binding was selective for gold. Quartz crystal microbalance studies show a strong

increase in the affinity of the peptide tagged protein over the native enzyme, while activity assays of protein bound to nanoparticles provide evidence that the enzyme retained catalytic activity when immobilized. In addition to showing selectivity, AFM images show significant differences in the height of the molecules when immobilized through the peptide tag compared to immobilization of the native enzyme, indicating differences in orientation of the bound enzyme when attached via the affinity tag. Controlling orientation of surface immobilized enzymes would further improve their enzymatic activity and impact diverse applications including oxidative biocatalysis, biosensors, biochips, and biofuel production.

Introduction

Nature has provided a versatile array of enzymes responsible for a wide variety of selective redox reactions. Oxidative enzymes have emerged as desirable for a range of applications due to their high degree of selectivity relative to other chemocatalysts.[1-3] This feature is highly valued by industry as the use of redox enzymes in organic synthesis can minimize by-product formation and circumvent the need for protection and deprotection steps.

Flavin-dependent oxidase enzymes in particular have been used extensively to generate compounds of interest to the pharmaceutical, chemical and agrochemical industries as well as for biosensing applications.[4-9] These enzymes contain a flavin adenine mononucleotide (FMN) or dinucleotide (FAD) which is tightly associated with the enzyme and, in some cases covalently bound.[1] Flavoprotein oxidases can catalyze two-electron oxidations of a wide range of compounds such as amines and alcohols, use molecular oxygen as an electron acceptor to generate hydrogen peroxide. Their ability to rely on the reductive activation of molecular oxygen as an electron acceptor to regenerate the oxidized enzyme-bound flavin provides a simpler and less expensive

system compared to other redox enzymes that require a constant supply of a dissociable coenzyme (nicotine amide dinucleotide (phosphate)/reduced nicotine amide dinucleotide (NAD(P)H/NADH)). Flavin oxidases that produce hydrogen peroxide are especially useful as the recognition element for biosensors since the hydrogen peroxide product is electroactive.[2-6]

The best studied flavin oxidase is glucose oxidase which has been applied for many years in the textile industry and for diagnostic applications.[7-9] Glucose oxidase catalyzes sugar oxidation coupled to the reduction of FAD to $FADH_2$ and to hydrogen peroxide production. Another flavin-containing enzyme is putrescine oxidase (PutOx, E.C 1.4.3.10) which is capable of degrading polyamines. PutOx is a homodimeric protein and unique among flavin-containing enzymes since the isolated enzyme appears to include only one non-covalently bound FAD per dimeric protein.[10-12] Recently, PutOx has been utilized as a diagnostic tool for the detection of biogenic amines such as putrescine and cadaverine[13-17] in body fluids as increased levels of these biogenic amines reflect tumor growth rates and thus can be used as tumor biomarkers.[18-19] PutOx is also used to monitor food freshness by detecting polyamines in spoiling food.[14, 20] The physiological and toxicological effects of several biogenic amines have been reported in a wide range of food products and are a potential public health concern. These include, but are not limited to, putrescine, histamine, cadaverine, spermine and agmatine. The consumption of foods containing high levels of biogenic amines has been associated with poisoning cases and health hazards; biogenic amines formed in food can cause serious allergic reactions that may lead to difficulty in breathing, itching, rash, vomiting, fever, and hypertension.[21-22] Consequently, there has been an increasing effort in developing sensors that allow monitoring of these compounds and relate the outcomes to the freshness of food products.[23] For instance, Inaba *et al* have developed an electrochemical biosensor based on two oxygen electrodes utilizing a combination of putrescine oxidase and agmatinase to

determine squid freshness.[14] Boka *et al* also developed a biosensor based on an enzyme modified carbon electrode for rapid determination of putrescine in food products with a detection limit of 0.01-0.25 mM.[13] Different immobilization techniques have been employed for putrescine biosensors. Enzyme electrodes were constructed by covalently binding the enzyme onto modified carbon or platinum surfaces by crosslinking with glutaraldehyde.[13, 17-18] Recently many efforts have been made to fabricate biosensors based on direct electron transfer between the catalytic site of enzyme and the electrode. This phenomenon is highly difficult in the case of PutOx, since the FAD cofactor is deeply embedded within the protein.[10-11] It is, however, feasible to create electron bridges between a conductive surface and a redox component within the enzyme, and this strategy is being actively pursued but again requires control over the surface orientation of the protein.

Immobilization of enzymes often results in reduction in stability and activity of the surface bound enzymes. Control over the orientation and the molecular level interactions at the solid support interfaces are the major contributors to such activity reductions. Biological systems typically integrate multicomponent self-assembly for complex tasks requiring precise function of many components working in tandem. There has been a growing interest in harnessing self-assembly in controlling molecular level interactions between enzymes and the surfaces. Yet, functional assembly of multicomponent systems at the nanoscale remains a significant challenge.[24-30] Incorporation of biomolecules into solid supports requires two critical considerations: 1) maintenance of functional integrity of the biomolecule when surface-immobilized, and 2) precise placement and orientation of the biomolecule in a manner that allows control over its interaction, not only with the interface directly but also with other components in the assembly.[31-32] These factors are essential for designing functional, complex, nanostructured materials and devices that involve proteins such as microarrays, biosensors, and biochips.[29-30, 32]

Self-assembled monolayers (SAM) that can be patterned using lithographic methods have been used extensively to create surface arrays of proteins for proteomic or biosensing applications.[33-38] Linkers that are most often used to immobilize proteins are silanes and thiols that bind at one end to the inorganic materials surface via silanol or thiol moieties and have a functional group at the other end (*e.g.* amine, carboxyl) for protein binding.[39-41] Although widely used, these linkers have a number of disadvantages including instability, lack of material selectivity or multilayer coverage. More importantly, attachment to surface groups on the protein is dependent on the availability and location of those groups. It is, therefore, difficult to control the orientation of the protein on the surface, which is often heterogeneous due to the attachment of the linker to one or more different groups on the surface of the protein. The variation due to such heterogeneous binding can result in a mixture of active, inactive, or partially active proteins on the surface.[25]

The use of surface-recognition peptides as an alternative to chemical coupling methods as surface specific bio-linkers is gaining considerable traction.[42-43] The peptides are selected from combinatorial peptide phage or cell surface display libraries. The peptide-mediated surface functionalization provides much greater control over the assembly process in a self-directed manner, removing the uncertainty of orientation that accompanies a random attachment approach where binding can occur through multiple sites on the protein. The dissociation constant values for surface-recognition peptides vary within the nM to mM range[44-46] and can be tuned for selective material binding over a wide range of surfaces.[47] The properties of these peptides have been critically examined in studies of surface functionalization, self-assembly, and formation of various nanostructures.[34-35] They were also demonstrated to be efficient surface linkers as fusion partners to other biomolecules.[48-50]

In the present work, we designed a self-immobilized biocatalyst system by focusing on a recently discovered putrescine oxidase from actinomycete *Rhodococcus erthropolis*. The enzyme (PutOx$_{Rh}$) displays a low level of sequence identity to other family members, but the structure of the flavin-binding region is highly conserved. PutOx$_{Rh}$ exhibits a high catalytic activity and high specificity toward putrescine as substrate ($k_{cat}/K_M = 3.2\times10^6$).[10] The enzyme is a homodimer with a molecular mass of ~100 kDa.[11] Flavin oxidases have been used in a variety of biosensing applications [13-15, 51-53] and the putrescine oxidase has been selected here as a model redox active enzyme for surface immobilization studies.[10, 13, 15] The most promising way to achieve direct electron transfer to a metal surface can be fusion of PutOx$_{Rh}$ enzyme with inorganic binding peptide, which is highly specific for several types of metal surfaces either flat or with structured nanoscale topography.[51, 54-58] In our prior work, we have demonstrated that the gold binding peptide alone binds to gold surfaces with high selectivity and affinity.[42-43] Building upon this prior work,[42-43] we have engineered a fusion protein consisting of the PutOx$_{Rh}$ and a C-terminal gold binding peptide (AuBP). We have chosen a novel putrescine oxidase identified from the genome of Rhodococcus erythropolis.[12] In this work, we have studied its assembly onto a both gold nanoparticles and flat Au(111) surfaces. The self-assembled PutOx-AuBP binds onto the gold surface with a significantly higher affinity than the native PutOx enzyme lacking the AuBP. We have also demonstrated that the immobilized enzyme remained functionally active when bound to the surface of gold nanoparticles. A detailed investigation of the enzyme binding using atomic force microscopy demonstrated that the protein shape and orientation at the surface are significantly altered on the gold surface upon the incorporation of the AuBP. The use of PutOx engineered with a peptide tag offers a precise assembly while securing the enzyme function in a

single step and can be adapted easily as a promising strategy for designing immobilized enzyme biocatalysts in multicomponent systems.

Experimental

Materials

DNA ligase and Dpn1 were purchased from Thermo Fisher Scientific. *E.coli* XL-10 Gold and BL21 (DE3) competent cells were purchased from Agilent Technologies. TEV was prepared as previously described.[59] NuPAGE gel, 12% Bis-Tris, Life Technologies, stained with InstantBlue from Expedeon. Gold-citrate nanoparticles were obtained Nanopartz™. All other reagents were of the highest grade available. Standard pH 8.0 phosphate buffer was obtained from Fisher scientific (10 mM Potassium phosphate monobasic/sodium hydroxide). Ruby muscovite mica was purchased from Lawrence Mica Company (New York). It was freshly cleaved before use. Milli-Q water (resistivity> 18.2 MΩ-cm) was used to rinse surfaces before and after protein incubation.

Template stripped gold surfaces were prepared by thermal evaporation of gold (Alfa Aesar, 99.999%) on mica at a rate of ~1-3 Å/sec in an Edwards Auto 306 thermal evaporator while heating to a temperature of ~200℃ with a quartz lamp. Template stripping was carried out as described previously.[60-62] Briefly, the samples were glued to a clean glass surface using Epo-Tek 377 epoxy (Epoxy Technology) and cured at 80℃ for 16 to 24 hours (h). The pieces were mechanically cleaved at the gold/mica interface immediately prior to use to expose a flat Au (111) surface with relatively large grains.

Expression vector construction

Construction of expression vectors for the production of PutOx-AuBP was performed using whole plasmid PCR mutagenesis on the pTBMalE plasmid[63] encoding the putrescine oxidase (PutOx) gene from *Rhodococcus erythropolis* together with His6-Maltose-Binding Protein (His6-MBP). Mutagenic PCR primers targeted to either the N or C terminus of the PutOx gene were produced with 5' overhangs each encoding half of the cyclic AuBP peptide (cpgWALRRSIRRQSYgpc) plus linker (PGGG) sequence.[12, 42, 44, 50] For the production of the N terminal construct, primer annealing sites were chosen to delete the MBP, and TEV cut site coding regions thereby generating an ORF coding for PutOx-AuBP. The annealing site of primers for C terminal insertion was selected to leave these sequences intact with the intention of removing them by TEV protease cleavage after expression. The primers used are shown in Table S1. Primers were phosphorylated on their 5' termini with polynucleotide kinase prior to PCR. PCR products were purified using a Qiagen PCR cleanup kit, ligated with DNA ligase, digested with Dpn1 and transformed into 50 μL of XL-10 Gold cells. Transformants were selected on 100 μg/mL ampicillin LB agar plates. DNA from transformant colonies was purified using a Qiagen miniprep kit, sequenced and transformed into BL21 (DE3) pRARE cells for expression. BL21 (DE3) pRARE cells were also transformed with the unmutated pTBMalE- PutOX expression vector for side by side production of the wild type enzyme.

Protein expression and purification

Transformant starter cultures of BL21 DE3 pRARE were grown in 25 mL Luria Bertani (LB) broth containing 200 μg/mL carbenicillin at 30^{o}C overnight. Large scale protein expression was performed the next day at 20^{o}C in 1 L of enhanced LB medium (200 μg/mL carbenicillin, 50 g

low salt LB mix, 10 mM $MgCl_2$, 0.8 % (V/V) glycerol, 89 mM sodium phosphate, pH 7.4). Cells were grown to an OD_{600} of 0.6 at 350 rpm shaking speed before the addition of 100 μM Isopropyl-B-D-1-thiogalactopyranoside (IPTG) and 0.5 % (V/V) glycerol. Expression was allowed to continue for 24 hours before cells were chilled to 4^{o}C and harvested by centrifugation at 2744 rcf for 10 min. Cell pellets were resuspended in 100 mL lysis buffer (50 mM Tris-HCl, pH 8.0, 300 mM NaCl, 10 mM imidazole) and frozen overnight at -80^{o}C. Cell suspensions were thawed and sonicated in an ice water bath using a Branson model 400 sonifier (2 sec on, 10 s off at 30% amplitude for 10 min). The lysate was clarified by centrifugation at 20,000 rcf for 1 hour. The soluble fraction was gently mixed with 5 mL of Qiagen Superflow Ni-NTA resin equilibrated with lysis buffer. The resin slurry was loaded onto a 1.6 cm x 30 cm (biorad) column and washed with 20 column volumes of lysis buffer followed by 20 column volumes of lysis buffer containing 20 mM imidazole. The protein was eluted with 1.5 column volumes of lysis buffer containing 250 mM imidazole-HCl.

The eluate from the Ni-NTA column was subjected to gel filtration on Sephadex G50 equilibrated with TEV protease buffer (10 mM Tris-HCl, pH 7.5, 100 mM NaCl, 100 μM EDTA, and 2 mM DTT). The TEV protease was added to a 1:20 (TEV: protein) molar ratio. The cleavage reactions were sterile filtered, and cleavage was allowed to proceed for 48 hours at 25^{o}C. Following gel filtration on Sephadex G50 equilibrated with TBS (20 mM Tris-HCl, pH 7.5, 140 mM NaCl), the protein was applied to a Ni-NTA column. The tag-less protein that was collected in the flow-through was >99% pure as judged by SDS-PAGE (Figure 1). The protein was concentrated to ~40 mg/mL by ultrafiltration (Amicon Ultra-15 concentrator) and loaded onto a 1.6 × 60 cm Superdex PG200 column at a flow rate of 1.25 mL/min. Peak fractions containing the

PutOx-AuBP or PutOx dimer were pooled, glycerol added to 20% (v/v), and the sample flash frozen in liquid nitrogen and stored at -80^{o}C.

Enzyme activity measurements

The putrescine oxidase activity was measured using a horseradish peroxidase (HRP)-coupled assay containing 2,2'-azino-bis (3-ethylbenzthiazoline-6-sulphonic acid) (ABTS) at 25^{o}C .[12] The hydrogen peroxide formed by PutOx is the primary substrate of HRP which couples the reduction of peroxide to the oxidation of ABTS, yielding a green chromogen that can be measured at 420 nm (ε_{420}=36000 μM^{-1} cm^{-1}). The standard assay mixture with HRP-ABTS consisted of 40 μM putrescine, 50 mM Tris HCl buffer at pH 8.0, 100 μM ABTS, 5 U HRP and 10 μl of the enzyme dilution sample. To determine the kinetic parameters, PutOx and/or PutOx-AuBP activities were measured at different putrescine concentrations (1 μM-40 μM) at 25^{o}C using HRP-ABTS enzyme assay through following the hydrogen peroxide formation by Cytation3 multimode spectrophotometer (Biotek, Vermont, USA). Data were then fitted with GraphPadPrism using the Michaelis-Menten equation for enzyme kinetics (Supporting Information, Fig. S1). Data were reproduced three times and all assays were performed in triplicates. The enzyme concentration was determined with the standard Bradford assay using bovine serum albumin (BSA) standards at 595 nm wavelength.

Gold nanoparticle binding assay

The activity of the PutOx and PutOx-AuBP bound to gold nanoparticles was analyzed by Amplex Red/Horseradish Peroxidase (HRP) assay after multiple washing steps to assess the robustness of the binding and activity. Efficient washing of nanoparticles was accomplished by

repeatedly collecting the particles by centrifugal sedimentation followed by withdrawal of a defined volume of the particle free supernatant and then resuspending the nanoparticle pellet in an equal volume of fresh buffer. Specifically, citrate capped gold nanoparticles were concentrated to 5 mg/mL by centrifugation at 200 x g for 48 h and resuspended in 100 μL H_2O. Aliquots of 25 μL of PutOx and PutOx-AuBP with a concentration of 10 mg/mL (100 μM) in 200 μM sodium phosphate buffer, pH 7.4, were combined with 25 μL of the concentrated nanoparticles and allowed to incubate at room temperature overnight with gentle mixing by inversion to prevent aggregation. Samples were then diluted with 900 μL of the sodium phosphate buffer and pelleted by centrifugation at 200 rcf for 48 h. A volume of 900 μL of the supernatant was carefully removed with a pipette and the pellet was resuspended in 50-100 μL of residual buffer. The protein/nanoparticle suspension was assayed for volume specific putrescine oxidation activity using the Amplex Red/Horseradish Peroxidase (HRP) assay method using 200 μM putrescine-HCl as the substrate. After resuspension and HRP activity assay (~20 min), 900 μL of phosphate washing buffer was added to the suspension and the particles were again collected by centrifugation. This cycle of washing the particles followed by volumetric specific activity determination was repeated 8 times.

Quartz crystal microbalance determination of binding constants

PutOx and PutOx-AuBP stock solutions were prepared for QCM-D analysis by gel filtration into 140 mM NaCl, 10 mM sodium phosphate, pH 7.4, followed by centrifugation at 21,000 rcf for 10 min and filtration through a 0.1 μm filter (Millipore, UltraFree-MC, type VV). The concentrations of protein samples were adjusted with freshly degassed buffer and filtered

through 0.2 μm Millipore filters. Amorphous gold QCM-D sensors (Q-sense) were rigorously cleaned, mounted in flow cells, and equilibrated with the same phosphate buffer for 2 hours. Only sensors achieving baseline stability (< 0.5 Hz/h drift) were used for data collection. Protein solutions were passed over the equilibrated sensors at 200 μL/min. For each concentration, side-by-side replicates were collected for both PutOx and PutOx-AuBP.

AFM imaging of protein on gold and mica

To study the material specificity of the proteins, template stripped gold and mica surfaces were used as substrates for protein adsorption. The surfaces were cleaned with pH adjusted (pH = 8.0) doubly distilled water for 45 seconds and conditioned with pH 8.0 phosphate buffer (10 mM potassium phosphate monobasic/sodium hydroxide) for 45 seconds. The protein concentrations were adjusted to 0.1 μM with the phosphate buffer. A volume of 100 μL of each protein sample was applied to the template stripped gold surfaces and mica surfaces and allowed to incubate for 2 hours. The surfaces were then washed with pH 8.0 phosphate buffer for 45 seconds, washed under a stream of pH adjusted MilliQ water (pH=8.0) for 45 seconds and dried under a stream of nitrogen. The surfaces were imaged after drying under nitrogen via tapping mode AFM *(Digital Instruments, NanoScope IIIa)*. Diamond-like carbon coated tips (TAP300DLC, *f=300 kHz, k = 40 N/m)* were used for imaging in tapping mode. Typical scan rates were 1 Hz with a scan size of 1 μm×1μm.

To determine the dimensions of single molecules, samples were prepared with low protein coverage. Protein solutions containing 0.01 μM PutOx-AuBP were allowed to adsorb for 15 min on template stripped gold surfaces followed by rinsing with buffer and water as described above. To isolate the unlabelled PutOx molecules on template stripped gold surfaces, a 0.1 μM solution of protein was incubated on the surface for 2 hours. For mica samples, 0.1 μM solutions were used

with 2 hours of incubation. (The higher protein concentration and longer incumbation times in these cases are due to the lower affinity, resulting in a smaller number of adsorbed molecules.) To measure the dimensions of individual molecules Bruker-NanoScope analysis 1.5 software was used, and from each sample, 50 molecules were analyzed over three different spots of the sample (n=50 for each protein). The average length and the width were measured as the full width at half maximum (FWHM) and the average height was measured with respect to the flat surface.

Results and discussion

Fusion protein constructs

The previously characterized gold binding peptide AuBP2[50] was chosen for this study due to its demonstrated high specificity and high affinity for binding to gold surfaces. The peptide was cyclized by incorporating flanking cysteinyl residues together with a short linker sequence attaching the peptide to the C-terminus of the protein. The oxidase partner for this construct, putrescine oxidase (PutOx), was chosen because it could be readily produced in a soluble, recombinant form when a maltose binding protein (MBP) solubility tag was incorporated into the N-terminus, plus a high resolution structure of the enzyme is available for computational analysis of constructs.[11] Preliminary experiments also indicated that PutOx retains >95% of its bound FAD upon purification following over-expression. Fusion proteins were engineered into the pTBMalE-4 vector such that they contained the AuBP on either the N- or the C-terminal end of the MBP-PutOx. When placed on the N-terminus of MBP-PutOx, attempts to recover the fusion protein from the soluble fraction, either by DEAE-cellulose or ammonium sulfate precipitation, resulted in irreversible aggregation of the protein. The N-terminally labeled construct was therefore abandoned. In contrast, when the AuBP was placed on the C-terminus of MBP-PutOx (see Fig.

1A) the fusion protein remained soluble during purification (see Fig. 1B) and retained 100% of its catalytic function when compared to the wild type enzyme (Fig. S1). A sequence coding for the TEV (tobacco etch virus) protease was introduced either 3′ (for N-terminal insertion) or 5’ (for C-terminal insertion) to the poly-linker insertion sites. This allowed the 6HisMBP tag to be cleaved from the protein following purification (see Fig. 1C and 1D). Several characterization methods were subsequently employed to examine the contribution of the AuBP to selective interaction with gold surfaces.

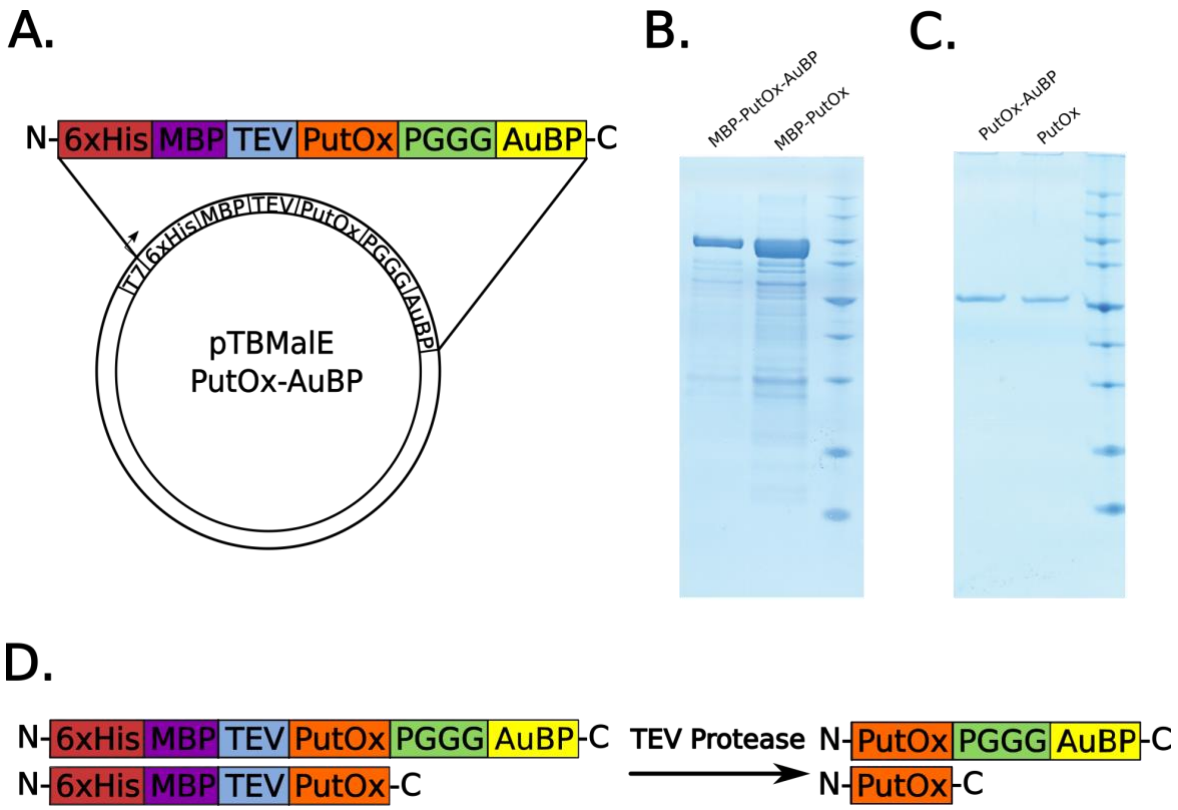

Figure 1. (A) Fusion protein construct in pTBMalE vector. (B) SDS-page gel of as expressed fusion construct with protein ladder (right lane). (C) SDS-page gel of protein after affinity column purification and cleavage of MBP. (D) TEV protease expected cleavage site.

Enzymatic activities of fusion protein

After the successful expression and purification of the engineered enzyme, PutOx-AuBP, the catalytic activity was tested. First the PutOx-AuBP's activity was first analyzed to elucidate its retention of catalytic activity following the insertion of the new gold binding domain, AuBP. The calculated kinetic parameters are provided in Table 1. The k_{cat}/K_m ratio, where k_{cat} is the catalytic constant for conversion of substrate into product, and K_m (Michaelis-Menten constant), which provides an estimation of the affinity of enzyme to its substrate and is defined as the substrate concentration at which initial rates are half of the maximum velocity has been widely used for enzyme efficiency. The k_{cat} value obtained for the PutOx-AuBP (25.5±0.8 s^{-1}) was determined to be comparable to that of wild type PutOx (26.4±0.5 s^{-1}), which indicates that the enzymatic conversion of putrescine is similar for both enzymes and the AuBP tag insertion did not influence the enzymatic activity. Similarly, the substrate affinities (K_m) of PutOx-AuBP and PutOx for putrescine were calculated to be comparable. The catalytic efficiency of the PutOx-AuBP was determined to be 92.7% of the wild type PutOx. Attained catalytic efficiency demonstrates the engineered PutOx-AuBP enzyme can be adapted as a robust self-assembling biocatalysis system.

Table 1. Steady-state kinetic parameters for putrescine of PutOx and PutOx-AuBP at pH 8.0

	***Km* (μM)**	***kcat* (s^{-1})**	***kcat/Km* ($s^{-1}mM^{-1}$)**
PutOx12	8.2±0.5	26.4±0.5	3200
PutOx-AuBP	8.6±0.7	25.5±0.8	2965

PutOx-AuBP attachment to gold nanoparticles

The enzyme (PutOx-AuBP or PutOx) was incubated for 2 hours with 15 nm diameter citrate-coated gold nanoparticles and then subjected to multiple centrifugal washes with phosphate buffer.

In this assay, nanoparticles are oversaturated with the proteins samples and the washing step removes free enzyme from solution, weakly bound protein, and reduces multi-layer formation of the enzyme over the nanoparticle surfaces (Fig. 2). The PutOx-AuBP is expected to replace the citrate on the particle surface as it binds. During adsorption, the particles were subjected to mixing overnight to prevent particle aggregation and multiple centrifugal washes were needed to completely remove the bulk excess unbound and weakly bound enzyme. At the end of each wash, the catalytic activity of the particles was measured using the Amplex red assay that measures the H_2O_2 generated upon putrescine oxidation.[64-65]The results indicated PutOx coated samples drastically continued to lose their activity starting from the 1st wash to complete loss of activity at the end of 8 washing cycles whereas PutOx-AuBP coated samples conserved more of their activity with steady levels of activity from the 3rd washing cycle until the end of the 8th cycle. The results indicate that AuBP peptide provided a tight binding to the engineered PutOx-AuBP biocatalysis system.

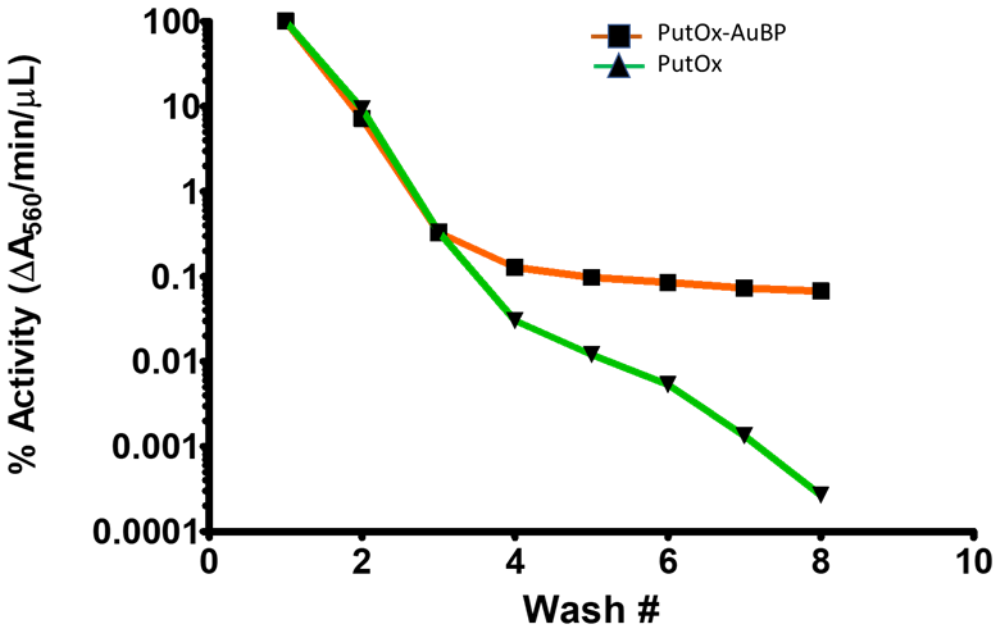

Figure 2. 15 nm diameter gold particles were incubated with wild type putrescene oxidase or PutOx-AuBP followed by successive wash cycles. Putrescene oxidase activity decreases in both cases, but more activity is retained in the case of the PutOx-AuBP. Activity is normalized to initial activity of protein bound particles.

QCM binding curves for the PutOx-AuBP fusion protein

The interaction between both PutOx-AuBP and PutOx and the gold surface were investigated using a quartz crystal microbalance. Protein binding to the gold surface was measured in a small flow cell at a constant flow rate of 200 μL/min and the frequency was recorded as a function of time. Multiple binding curves were collected using solutions with different protein concentrations. Response curves are shown for two different concentrations (20 nM and 100 nM) of PutOx-AuBP compared to 100 nM PutOx lacking the gold binding tag (see Fig. 3A). Adsorption data were fit to a single exponential to obtain maximum equilibrium frequency shift (Δf) values over a range of concentrations (see Fig. 3B). Little if any desorption occurred following several hours of washing in the absence of enzyme, indicating very tight binding. Estimates of the dissociation constant for binding of PutOx-AuBP were obtained from a Langmuir fit of the kinetic data (20.2 ± 9.6 nM)[66] as well as from a non-linear regression analysis (20.0 ± 7.1 nM) of the data shown in Figure 3B.

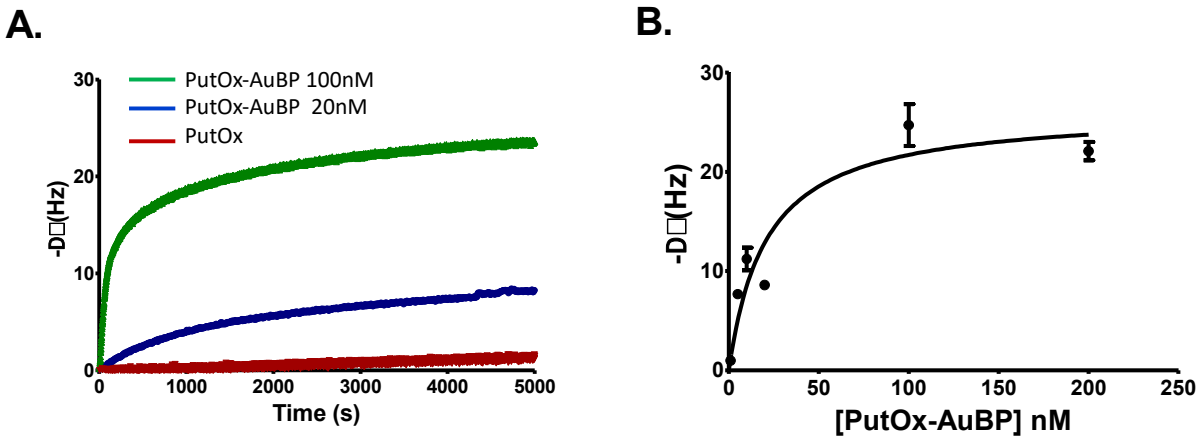

Figure 3. (A) QCM response curves (change in frequency vs time) for binding of PutOx(red) and PutOx-AuBP (blue at 20 nM, and green at 100 nM). (B) Concentration dependence of PutOx-AuBP binding.

The expression of the folded, functional, active protein with the peptide tag on the C-terminal end of the protein was demonstrated, while expression with the tag on the N-terminal end of the protein did not allow recovery of folded, active protein. Therefore, the tag was included on the C-terminus of the protein. The binding of the protein to gold nanoparticles and their stability under a series of washing steps showed that while both the native PutOx and the PutOx-AuBP bound to the gold nanoparticles and desorbed after washing steps, the PutOx-AuBP retained significantly more activity on the particles over time than did the PutOx. This is likely due to the higher affinity of the PutOx-AuBP for the gold, and possibly an increased stability of the PutOx-AuBP on the surface due to differences in binding. The difference in affinity for the gold was confirmed by QCM studies which showed much stronger binding of the PutOx-AuBP to the gold than the PutOx. In addition, the binding curves for the PutOx-AuBP show very little desorption of the protein from the surface when the protein solution was exchanged for the buffer only solution within the timeframe of the experiment (not shown), suggesting a very small k_d for this binding interaction. Analysis of the PutOx-AuBP/Au interaction indicated that the equilibrium binding constant (K_d) for the interaction is approximately 20 nM.

The binding and orientation of proteins at interfaces are critical for a variety of applications including biosensing and biocatalysis. In this work, the QCM and nanoparticle binding assays suggest that significant differences arise in the binding of the PutOx enzyme on gold surfaces, due to the incorporation of a relatively small peptide tag. Typically, these peptides are developed through biocombinatorial approaches including phage display to identify peptides with high

affinity for a particular surface. Genetically engineered peptide sequences have been developed for a variety of materials including gold, silver, platinum, silica, and graphite. They have been shown to control the direction of protein binding at the microscale, however little is known about the control of the orientation of the assembled proteins. Here, the binding of the PutOx has been specifically studied with and without the AuBP tag to investigate the role of the peptide tag in the binding process.

Protein coverage and orientation - AFM

The binding studies using QCM and nanoparticle washing experiments indicated that the PutOx-AuBP bound considerably more tightly to gold surfaces than the enzyme lacking the AuBP tag. To probe this binding further, the PutOx and PutOx-AuBP were introduced to template-stripped gold surfaces and mica surfaces. Protein films were imaged using AFM in air after protein adsorption for 2 hours at a concentration of 10 μg/mL. The images were collected in tapping mode under ambient conditions after washing with buffer and MilliQ water followed by drying with nitrogen (see Fig. 4). In Fig. 4A, the image shows the PutOx-AuBP on Au (111). This surface has a high coverage of protein molecules compared to the very low coverage indicated in the image of the PutOx (see Fig. 4C). This is consistent with the PutOx-AuBP molecules adsorbing to the surface via the AuBP tag. In contrast, on mica, the adsorption of the PutOx-AuBP and the PutOx under conditions identical to those for binding to the gold surface are relatively low and indistinguishable from one another. The coverage is identical, and the distribution of the two different protein molecules is similar on the mica surface indicating that the interaction with the mica surface is not affected by the presence of the AuBP.

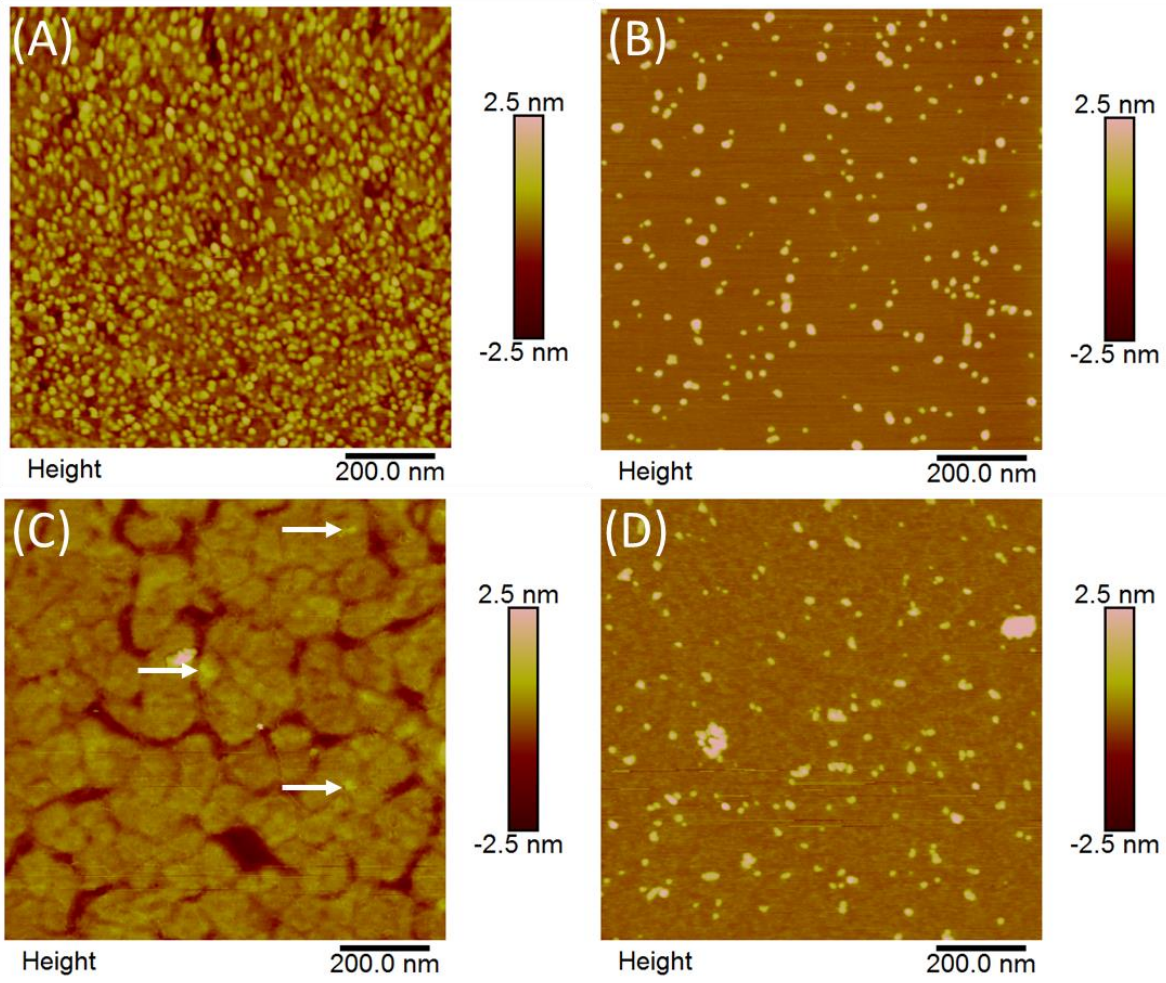

Figure 4. AFM images under ambient conditions of PutOx on Au(111) (A,C) and mica (B,D) surfaces. (A) PutOx-AuBP on Au(111) (B) PutOx-AuBP on mica (C) PutOx on Au(111), (D) PutOx on mica. The white arrows show some of the PutOx molecules on figure c.

Under low coverage conditions, AFM images of individual molecules can be analyzed to determine the single molecule dimensions of the protein. Representative images are shown in Fig. 5 along with cross-sectional profiles through the PutOx and the PutOx-AuBP molecules bound to gold. For each sample, 50 molecules were analyzed to determine the length, width (FWHM) and height of the molecules. The dimensions are reported in supplementary data (Table S3). As shown in Fig. 6, while there is little change in the length and width of the PutOx and the PutOx-AuBP, there is a significant increase in the height of the PutOx-AuBP molecules on Au compared to the

PutOx. The dimensions reported here have not been deconvoluted for the tip shape, but images were recorded with the same tip under similar imaging conditions to allow direct comparison. When a similar analysis is carried out for the individual molecules on the mica surface, there is no significant difference in any of the three dimensions, again suggesting that the adsorption of the PutOx to mica is not affected by the presence of the AuBP tag, but the adsorption to gold is significantly modified. The increase in height of approximately 1 nm observed on the Au surface of bound PutOx-AuBP is significant and likely comes from a difference in how the protein is interacting with the surface. This suggests that the presence of the AuBP holds the protein away from the surface in a more vertical orientation. The significant increase in coverage of the PutOx-AuBP on Au is consistent with this difference in interaction as well as the tighter binding observed between the PutOx-AuBP and the Au in the QCM data.

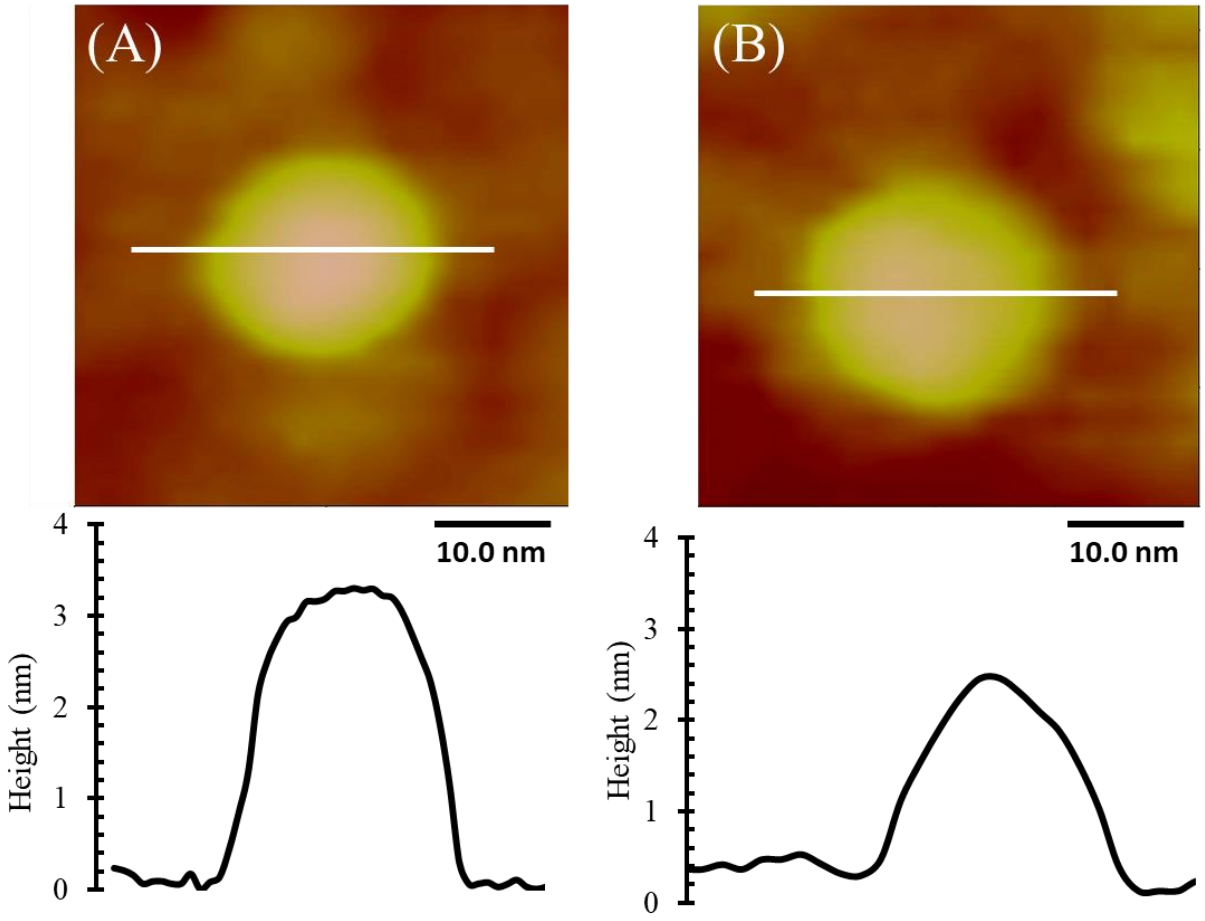

Figure 5. AFM images of individual molecules on the Au(111) surface along with cross-sectional profiles through the molecules along the indicated line in the image. (A) PutOx-AuBP (B) PutOx.

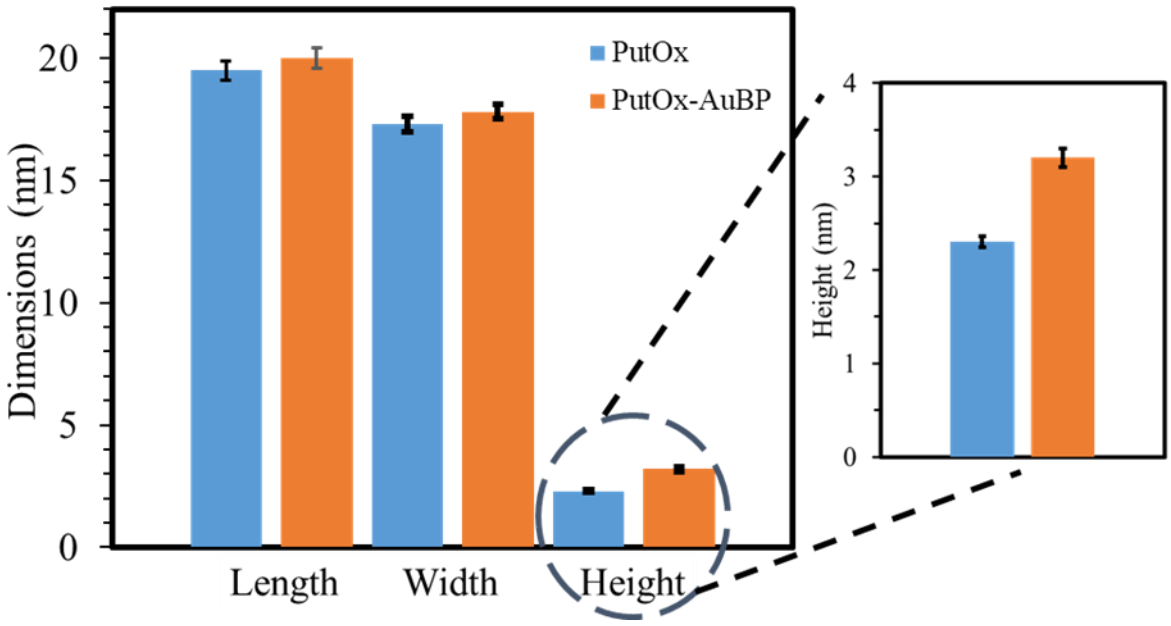

Figure 6. AFM measured dimensions of PutOx-AuBP and PutOx on Au(111). The dimensions are from a single sample, at three different locations and experiment has been replicated three times with similar results. Error bars represent 95% confidence limits based on the analysis of n=50 molecules.

These data provide a clear link between single molecule shape and orientation and protein binding using these peptide tags. In contrast, when similar experiments were carried out on mica surfaces, there was no change in coverage or dimensions of the protein when the AFM experiments were carried out. This confirms that the differences seen between the PutOx and PutOx-AuBP binding on the gold surface are in fact due to the specific interaction between the peptide tag and the gold surface. Similar experiments have been conducted on other surfaces as well and will be the subject of a future manuscript. The fact that the binding through the AuBP tag results in significant differences in not only the protein coverage, but also the shape and orientation suggests that binding through these genetically engineered peptide tags may provide strong benefits in protein assembly at interfaces over other methods for peptide attachment, including nonspecific

interactions (both covalent and noncovalent coupling) which lack the precise control of orientation and materials specificity desired. Facile, self-assembly of complex multicomponent systems necessitates material specificity as well as orientational control that binding through the engineered peptide tags affords.

Conclusion

Flavin oxidases are responsible for catalyzing the oxidation of diverse analytes with hydrogen peroxide as a product. Hydrogen peroxide production is often used as a measure of catalytic activity, making flavin oxidases attractive targets for biosensing applications. The ability of flavin oxidases to use molecular oxygen as an electron acceptor makes these enzymes industrially attractive as they are inexpensive and straightforward enzymes compared to other redox enzymes. Here, we engineered a novel flavin containing oxidase from *Rhodococcus erythropolis* NCIMB 11540, putrescine oxidase (PutOx) which is used to monitor the degradation of biogenic amines for applications such as food spoilage and tumor biomarker detection. The detection of the electron transfer reaction in the putrescine oxidase is challenging due to the location of the flavin adenine dinucleotide (FAD) site in the protein. Controlling the orientation to provide an active conformation of the protein at the interface will impact the wider implementation of such enzymes as useful biocatalysts. To address this critical issue, we have investigated the self-assembly of PutOx on gold surfaces using a gold binding peptide, AuBP, to guide the enzyme orientation by providing a competitive binding site. The expression and purification of the novel PutOx-AuBP engineered enzyme with near native activity was demonstrated. In addition, standard activity assays showed that the functional activity of the tagged enzyme was comparable to that of the wild type enzyme. Engineered enzyme coated nanoparticles remained active on the surface

after several washing cycles, whereas the activity of the wild type enzyme decreased much more rapidly with repeated washing. Binding studies using QCM spectroscopy demonstrated that the PutOx-AuBP construct bound to gold surface with higher affinity than the native PutOx. Analysis of AFM images showed that the PutOx-AuBP resulted in a higher coverage on the surface than the native PutOx under identical adsorption conditions. In addition, single molecule AFM measurements at low coverage revealed a significant difference in the height of the PutOx-AuBP and the native PutOx on the gold surface, while no such difference was observed in the case of adsorption on a mica surface. The specific attachment of functionally active PutOx via the AuBP to gold surfaces has been demonstrated using a combination of QCM, activity assays, and AFM investigations of coverage and shape of individual molecules. The increase in coverage as well as the difference in single molecule dimensions show that the binding to the gold surface is mediated by a specific interaction with the AuBP, which results in a more stably bound, functionally active protein at the interface with a different shape than enzyme bound nonspecifically without the AuBP. This highlights the critical role of controlling specific interfacial interactions when self-assembling proteins at interfaces for an expanding list of applications of hybrid nanodevices based on proteins. Specifically, these studies demonstrate the potential for the control of binding, assembly, and orientation of active PutOx on the surface which should allow the design of much more sensitive and robust biocatalysts as well as biosensor systems based on the flavoprotein oxidases. Moreover, the technique should be readily adaptable to other enzyme systems for which it is difficult to develop a suitable biosensor platform.

Supporting information

Additional information is provided for the mutagenic whole plasmid PCR primers, AFM measured dimensions of PutOx-AuBP and PutOx on Au(111) and Michaelis-Menten plot of engineered enzyme, PutOx-AuBP.

Acknowledgments

This work was supported by the Strategic Initiative Grant from the University of Kansas and The Scientific and Technological Research Council of Turkey (TUBITAK) through a 2214-A Scholar Program (Banu Taktak Karaca) and NIH graduate training grant 5T32GM008359-27 (Dwight Deay III).

References

1. Torres Pazmiño, D. E.; Winkler, M.; Glieder, A.; Fraaije, M. W., Monooxygenases as biocatalysts: classification, mechanistic aspects and biotechnological applications. *J Biotechnol* **2010,** *146* (1-2), 9-24.
2. Ceccoli, R. D.; Bianchi, D. A.; Rial, D. V., Flavoprotein monooxygenases for oxidative biocatalysis: recombinant expression in microbial hosts and applications. *Front. Microbiol.* **2014,** *5*, 1-14.
3. Dong, J. J.; Fernández-Fueyo, E.; Hollmann, F.; Paul, C. E.; Pesic, M.; Schmidt, S.; Wang, Y.; Younes, S.; Zhang, W., Biocatalytic oxidation reactions: a chemist's perspective. *Angew. Chem. Int. Ed.* **2018,** *57*, 9238-9261.
4. Montersino, S.; Tischler, D.; Gassner, G. T.; Van Berkel, W. J. H., Catalytic and structural features of flavoprotein hydroxylases and epoxidases. *Adv Synth Catal* **2011,** *353*, 2301-2319.
5. Moonen, M. J. H.; Fraaije, M. W.; Rietjens, I. M. C. M.; Laane, C.; Van Berkel, W. J. H., Flavoenzyme-Catalyzed Oxygenations and Oxidations of Phenolic Compounds. *Adv Synth Catal* **2002,** *344*, 1023-1035.
6. Ullrich, R.; Hofrichter, M., Enzymatic hydroxylation of aromatic compounds. *Cell Mol Life Sci* **2007,** *64* (3), 271-293.
7. Bankar, S. B.; Bule, M. V.; Singhal, R. S.; Ananthanarayan, L., Glucose oxidase - An overview. *Biotechnol. Adv* **2009,** *27* (4), 489-501.
8. Tzanov, T.; Costa, S. A.; Gbitz, G. M.; Cavaco-Paulo, A., Hydrogen peroxide generation with immobilized glucose oxidase for textile bleaching. *J Biotechnol* **2002,** *93* (1), 87-94.
9. Wilson, R.; Turner, A. P. F., Glucose oxidase: an ideal enzyme. *Biosens. Bioelectron.* **1992,** *7* (3), 165-85.
10. Kopacz, M. M.; Heuts, D. P. H. M.; Fraaije, M. W., Kinetic mechanism of putrescine oxidase from Rhodococcus erythropolis. *FEBS Journal* **2014,** *281* (19), 4384-4393.
11. Kopacz, M. M.; Rovida, S.; van Duijn, E.; Fraaije, M. W.; Mattevi, A., Structure-based redesign of cofactor binding in putrescine oxidase. *Biochemistry* **2011,** *50* (19), 4209-17.
12. Van Hellemond, E. W.; Van Dijk, M.; Heuts, D. P. H. M.; Janssen, D. B.; Fraaije, M. W., Discovery and characterization of a putrescine oxidase from Rhodococcus erythropolis NCIMB 11540. *Appl. Microbiol.* **2008,** *78* (3), 455-463.
13. Bka, B.; Adnyi, N.; Szamos, J.; Virg, D.; Kiss, A., Putrescine biosensor based on putrescine oxidase from Kocuria rosea. *Enzyme Microb. Technol.* **2012,** *51* (5), 258-262.
14. Inaba, Y.; Tokishita, S.; Hamada-Sato, N.; Kobayashi, T.; Imada, C.; Yamagata, H.; Watanabe, E., Development of agmatine sensor using the combination of putrescine oxidase and agmatinase for squid freshness. *Biosens. Bioelectron.* **2004,** *20* (4), 833-840.
15. Lee, J. I.; Jang, J. H.; Yu, M. J.; Kim, Y. W., Construction of a bifunctional enzyme fusion for the combined determination of biogenic amines in foods. *Agric. Food Chem.* **2013,** *61* (38), 9118-9124.
16. Nagy, L.; Nagy, G.; Gyurcsnyi, R. E.; Neuman, M. R.; Lindner, E., Development and study of an amperometric biosensor for the in vitro measurement of low concentration of putrescine in blood. *J Biochem Bioph Meth* **2002,** *53* (1-3), 165-175.
17. Rochette, J. F.; Sacher, E.; Meunier, M.; Luong, J. H. T., A mediatorless biosensor for putrescine using multiwalled carbon nanotubes. *Anal. Biochem.* **2005,** *336* (2), 305-311.

18. Casero, R. A.; Marton, L. J., Targeting polyamine metabolism and function in cancer and other hyperproliferative diseases. *Nat. Rev. Drug Discov.* **2007,** *6* (5), 373-390.
19. Liu, R.; Lin, X.; Li, Z.; Li, Q.; Bi, K., Quantitative metabolomics for investigating the value of polyamines in the early diagnosis and therapy of colorectal cancer. *Oncotarget* **2018,** *9* (4), 4583-4592.
20. Kalač, P.; Krausová, P., A review of dietary polyamines: Formation, implications for growth and health and occurrence in foods. *Food Chem.* **2005,** *90* (1-2), 219-230.
21. Bardcz, S., Polyamines in food and their consequences for food quality and human health. *Trends Food Sci. Tech.* **1995,** *6* (10), 341-346.
22. Kalač, P., Health effects and occurrence of dietary polyamines: A review for the period 2005-mid 2013. *Food Chem.* **2014,** *161*, 27-39.
23. Reverte, L.; Prieto-Simon, B.; Campas, M., New advances in electrochemical biosensors for the detection of toxins: Nanomaterials, magnetic beads and microfluidics systems. A review. *Anal Chim Acta* **2016,** *908*, 8-21.
24. Muguruma, H.; Iwasa, H.; Hidaka, H.; Hiratsuka, A.; Uzawa, H., Mediatorless direct electron transfer between flavin adenine dinucleotide-dependent glucose dehydrogenase and single-walled carbon nanotubes. *ACS Catalysis* **2017,** *7* (1), 725-734.
25. Sarikaya, M.; Tamerler, C.; Schwartz, D. T.; Baneyx, F., Materials assembly and formation using engineered polypeptides. *Annu. Rev. Mater. Res.* **2004,** *34*, 373-408.
26. Schulz, C.; Kittl, R.; Ludwig, R.; Gorton, L., Direct electron transfer from the FAD cofactor of cellobiose dehydrogenase to electrodes. *ACS Catalysis* **2016,** *6* (2), 555-563.
27. So, C. R.; Kulp, J. L.; Oren, E. E.; Zareie, H.; Tamerler, C.; Evans, J. S.; Sarikaya, M., Molecular recognition and supramolecular self-assembly of a genetically engineered gold binding peptide on Au(111). *ACS Nano* **2009,** *3* (6), 1525-1531.
28. Tamerler, C.; Sarikaya, M., Molecular biomimetics: genetic synthesis, assembly, and formation of materials using peptides. *MRS Bulletin* **2008,** *33* (5), 504-512.
29. Willner, I., Biomaterials for sensors, fuel cells, and circuitry. *Science* **2002,** *298*, 2407-2409.
30. Willner, I.; Willner, B., Biomolecule-based nanomaterials and nanostructures. *Nano Lett.* **2010,** *10*, 3805-3815.
31. Tamerler, C.; Duman, M.; Oren, E. E.; Gungormus, M.; Xiong, X.; Kacar, T.; Parviz, B. A.; Sarikaya, M., Materials specificity and directed assembly of a gold-binding peptide. *Small* **2006,** *2* (11), 1372-1378.
32. Woodbury, R. G.; Wendin, C.; Clendenning, J.; Melendez, J.; Elkind, J.; Bartholomew, D.; Brown, S.; Furlong, C. E., Construction of biosensors using a gold-binding polypeptide and a miniature integrated surface plasmon resonance sensor. *Biosens. Bioelectron.* **1998,** *13* (10), 1117-1126.
33. Haussmann, A.; Milde, P.; Erler, C.; Eng, L. M., Ferroelectric lithography: Bottom-up assembly and electrical performance of a single metallic nanowire. *Nano Lett.* **2009,** *9* (2), 763-768.
34. Hnilova, M.; Khatayevich, D.; Carlson, A.; Oren, E. E.; Gresswell, C.; Zheng, S.; Ohuchi, F.; Sarikaya, M.; Tamerler, C., Single-step fabrication of patterned gold film array by an engineered multi-functional peptide. *J. Colloid Interface Sci.* **2012,** *365* (1), 97-102.
35. Kacar, T.; Zin, M. T.; So, C.; Wilson, B.; Ma, H.; Gul-Karaguler, N.; Jen, A. K.; Sarikaya, M.; Tamerler, C., Directed self-immobilization of alkaline phosphatase on micro-patterned

substrates via genetically fused metal-binding peptide. *Biotechnol. Bioeng.* **2009,** *103* (4), 696-705.
36. David S. Ginger, H. Z., and Chad A. Mirkin, The evolution of dip-Pen nanolithography. *Angew. Chem. Int. Ed.* **2004,** *43*, 30-45.
37. Khalid Salaita, Y. W., Chad A. Mirkin, Applications of dip-pen nanolithography. *Nat. Nanotechnol.* **2007,** *2*, 146-155.
38. Joydeep Lahiri, E. O., and George M. Whitesides, Patterning ligands on reactive SAMs by microcontact printing. *Langmuir* **1999,** *15*, 2055-2060.
39. Fenter, P.; Eisenberger, P.; Li, J.; Camillone, N.; Bernasek, S.; Scoles, G.; Ramanarayanan, T. A.; Liang, K. S., Structure of $CH_3(CH_2)_{17}SH$ Self-assembled on the Ag(111) surface: an incommensurate monolayer. *Langmuir* **1991,** *7* (10), 2013-2016.
40. Leong, K.; Chen, Y.; Masiello, D. J.; Zin, M. T.; Hnilova, M.; Ma, H.; Tamerler, C.; Sarikaya, M.; Ginger, D. S.; Jen, A. K. Y., Cooperative near-field surface plasmon enhanced quantum dot nanoarrays. *Adv. Funct. Mater.* **2010,** *20* (16), 2675-2682.
41. Porter, M. D.; Bright, T. B.; Allara, D. L.; Chidsey, C. E., Spontaneously organized molecular assemblies. 4. structural characterization of n-alkyl thiol monolayers on gold by optical ellipsometry, infrared spectroscopy, and electrochemistry. *J. Am. Chem. Soc.* **1987,** *109* (12), 3559-3568.
42. Sarikaya, M.; Aksay, I. A., Biomimetics : design and processing of materials. In *AIP series in polymers and complex materials*, 1995; pp 147-160.
43. So, C. R.; Hayamizu, Y.; Yazici, H.; Gresswell, C.; Khatayevich, D.; Tamerler, C.; Sarikaya, M., Controlling self-assembly of engineered peptides on graphite by rational mutation. *ACS Nano* **2012,** *6* (2), 1648-56.
44. Akdim, B.; Pachter, R.; Kim, S. S.; Naik, R. R.; Walsh, T. R.; Trohalaki, S.; Hong, G.; Kuang, Z.; Farmer, B. L., Electronic properties of a graphene device with peptide adsorption: Insight from simulation. *ACS Appl. Mater. Interfaces* **2013,** *5* (15), 7470-7477.
45. Sarikaya, M.; Tamerler, C.; Jen, A. K. Y.; Schulten, K.; Baneyx, F., Molecular biomimetics: Nanotechnology through biology. *Nat. Mater.* **2003,** *2*, 577-585.
46. Tamerler, C.; Khatayevich, D.; Gungormus, M.; Kacar, T.; Oren, E. E.; Hnilova, M.; Sarikaya, M., Molecular biomimetics: GEPI-based biological routes to technology. *Biopolymers* **2010,** *94* (1), 78-94.
47. Evans, J. S.; Samudrala, R.; Walsh, T. R.; Oren, E. E.; Tamerler, C., Molecular design of inorganic-binding polypeptides. *MRS Bulletin* **2008,** *33* (5), 514-518.
48. Hnilova, M.; Karaca, B. T.; Park, J.; Jia, C.; Wilson, B. R.; Sarikaya, M.; Tamerler, C., Fabrication of hierarchical hybrid structures using bio-enabled layer-by-layer self-assembly. *Biotechnol. Bioeng.* **2012,** *109* (5), 1120-1130.
49. Hnilova, M.; Liu, X.; Yuca, E.; Jia, C.; Wilson, B.; Karatas, A. Y.; Gresswell, C.; Ohuchi, F.; Kitamura, K.; Tamerler, C., Multifunctional protein-enabled patterning on arrayed ferroelectric materials. *ACS Appl. Mater. Interfaces* **2012,** *4* (4), 1865-1871.
50. Hnilova, M.; So, C. R.; Oren, E. E.; Wilson, B. R.; Kacar, T.; Tamerler, C.; Sarikaya, M., Peptide-directed co-assembly of nanoprobes on multimaterial patterned solid surfaces. *Soft Matter* **2012,** *8* (16), 4327-4334.
51. Hu, Y.; Mitchell, K. M.; Albahadily, F. N.; Michaelis, E. K.; Wilson, G. S., Direct measurement of glutamate release in the brain using a dual enzyme-based electrochemical sensor. *Brain Research* **1994,** *659* (1-2), 117-125.

52. Wilson, G. S.; Gifford, R., Biosensors for real-time in vivo measurements. *Biosens. Bioelectron.* **2005,** *20* (12), 2388-2403.
53. Wilson, G. S.; Hu, Y., Enzyme-based biosensors for in vivo measurements. *Chem. Rev* **2000,** *100* (7), 2693-2704.
54. Karaca, B. T.; Hnilova, M.; Tamerler, C., Addressable biological functionalization of inorganics: Materials-selective fusion proteins in bio-nanotechnology. In *Bio-Inspired Nanotechnology*, Springer: New York, 2014; pp 221-255.
55. VanOosten, S. K.; Yuca, E.; Karaca, B. T.; Boone, K.; Snead, M. L.; Spencer, P.; Tamerler, C., Biosilver nanoparticle interface offers improved cell viability. *Surf Innov* **2016,** *4* (3), 121-132.
56. Yuca, E.; Karatas, A. Y.; Seker, U. O. S.; Gungormus, M.; Dinler-Doganay, G.; Sarikaya, M.; Tamerler, C., In vitro labeling of hydroxyapatite minerals by an engineered protein. *Biotechnol. Bioeng.* **2011,** *108* (5), 1021-1030.
57. Yucesoy, D. T.; Karaca, B. T.; Cetinel, S.; Caliskan, H. B.; Adali, E.; Gul-Karaguler, N.; Tamerler, C., Direct bioelectrocatalysis at the interfaces by genetically engineered dehydrogenase. *Bioinspir. Biomim. Nan.* **2015,** *4* (1), 79-89.
58. Zhang, S.; Karaca, B. T.; Vanoosten, S. K.; Yuca, E.; Mahalingam, S.; Edirisinghe, M.; Tamerler, C., Coupling infusion and gyration for the nanoscale assembly of functional polymer nanofibers integrated with genetically engineered proteins. *Macromol. Rapid Commun.* **2015,** *36* (14), 1322-1328.
59. Tropea, J. E.; Cherry, S.; Waugh, D. S., Expression and purification of soluble His(6)-tagged TEV protease. *Methods Mol Biol* **2009,** *498*, 297-307.
60. Vogel, N.; Zieleniecki, J.; Köper, I., As flat as it gets: ultrasmooth surfaces from template-stripping procedures. *Nanoscale* **2012,** *4*, 3820-3832.
61. Wagner, P.; Hegner, M.; Guntherodt, H.-J.; Semenza, G., Formation and in Situ Modification of Monolayers Chemisorbed on Ultraflat Template-Stripped Gold Surfaces. *Langmuir* **1995,** *11*, 3867-3875.
62. Hegner, M.; Wagner, P.; Semenza, G., Ultralarge atomically flat template-stripped Au surfaces for scanning probe microscopy. *Surface Science* **1993,** *291*, 39-46.
63. Hu, J.; Qin, H.; Gao, F. P.; Cross, T. A., A systematic assessment of mature MBP in membrane protein production: overexpression, membrane targeting and purification. *Protein Expr Purif* **2011,** *80* (1), 34-40.
64. Mishin, V.; Gray, J. P.; Heck, D. E.; Laskin, D. L.; Laskin, J. D., Application of the Amplex red/horseradish peroxidase assay to measure hydrogen peroxide generation by recombinant microsomal enzymes. *Free Radic. Biol. Med.* **2010,** *48* (11), 1485-1491.
65. Zhou, M.; Diwu, Z.; Panchuk-Voloshina, N.; Haugland, R. P., A stable nonfluorescent derivative of resorufin for the fluorometric determination of trace hydrogen peroxide: applications in detecting the activity of phagocyte NADPH oxidase and other oxidases. *Anal. Biochem.* **1997,** *253* (2), 162-168.
66. Tamerler, C.; Oren, E. E.; Duman, M.; Venkatasubramanian, E.; Sarikaya, M., Adsorption kinetics of an engineered gold binding Peptide by surface plasmon resonance spectroscopy and a quartz crystal microbalance. *Langmuir* **2006,** *22* (18), 7712-8.

Table of Contents Graphic